Supplementary material
for
An assessment of the Arctic Ocean in a suite of interannual CORE-II simulations. Part II: Liquid freshwater

Qiang Wang[a,*], Mehmet Ilicak[b], Rüdiger Gerdes[a], Helge Drange[c], Yevgeny Aksenov[d], David A Bailey[e], Mats Bentsen[b], Arne Biastoch[f], Alexandra Bozec[g], Claus Böning[f], Christophe Cassou[h], Eric Chassignet[g], Andrew C. Coward[d], Beth Curry[i], Gokhan Danabasoglu[e], Sergey Danilov[a], Elodie Fernandez[h], Pier Giuseppe Fogli[j], Yosuke Fujii[k], Stephen M. Griffies[l], Doroteaciro Iovino[j], Alexandra Jahn[e,m], Thomas Jung[a,n], William G. Large[e], Craig Lee[i], Camille Lique[o], Jianhua Lu[g], Simona Masina[j], A.J. George Nurser[d], Benjamin Rabe[a], Christina Roth[f], David Salas y Mélia[p], Bonita L. Samuels[l], Paul Spence[q,r], Hiroyuki Tsujino[k], Sophie Valcke[h], Aurore Voldoire[p], Xuezhu Wang[a], Steve G. Yeager[e]

[a] *Alfred Wegener Institute, Helmholtz Centre for Polar and Marine Research (AWI), Bremerhaven, Germany*
[b] *Uni Research Ltd., Bergen, Norway*
[c] *University of Bergen, Bergen, Norway*
[d] *National Oceanography Centre (NOC), Southampton, SO14 3ZH, UK*
[e] *National Center for Atmospheric Research (NCAR), Boulder, CO, USA*
[f] *GEOMAR Helmholtz Centre for Ocean Research, Kiel, Germany*
[g] *Center for Ocean-Atmospheric Prediction Studies (COAPS), Florida State University, Tallahassee, FL, USA*
[h] *Centre Européen de Recherche et de Formation Avancée en Calcul Scientifique (CERFACS), Toulouse, France*
[i] *Applied Physics Laboratory, University of Washington, seattle, Washington, USA*
[j] *Centro Euro-Mediterraneo sui Cambiamenti Climatici (CMCC), Bologna, Italy*
[k] *Meteorological Research Institute (MRI), Japan Meteorological Agency, Tsukuba, Japan*
[l] *NOAA Geophysical Fluid Dynamics Laboratory (GFDL), Princeton, NJ, USA*
[m] *Department of Atmospheric and Oceanic Sciences, University of Colorado, Boulder, CO, USA*
[n] *Institute of Environmental Physics, University of Bremen, Bremen, Germany*
[o] *Department of Earth Sciences, University of Oxford, Oxford, UK*
[p] *Centre National de Recherches Météorologiques (CNRM), Toulouse, France*
[q] *Climate Change Research Centre, University of New South Wales, Sydney, Australia*
[r] *ARC Centre of Excellence for Climate System Science, University of New South Wales, Sydney, Australia*

1. Correlation coefficients between models

The plots of correlation coefficients between the CORE-II models for different terms of Arctic freshwater (FW) budget are collected in Figures 1 and 2. These plots support the discussion in Section 3.

2. Ocean volume transport variability at Davis Strait

The interannual variability of ocean volume transport through Davis Strait is discussed in details in this section.

Background

Because of the impact of Arctic freshwater (FW) export on the North Atlantic, many studies have focused on the mechanisms driving the variability of the FW export. Studies over the last decade have significantly improved the understanding on the variability of Canadian Arctic Archipelago (CAA) throughflow by using observations (Prinsenberg and Hamilton, 2005; Prinsenberg et al., 2009; Peterson et al., 2012) and ocean model simulations (Condron et al., 2009; Jahn et al., 2010a,b; Houssais and

*Corresponding author
Email address: Qiang.Wang@awi.de (Qiang Wang)

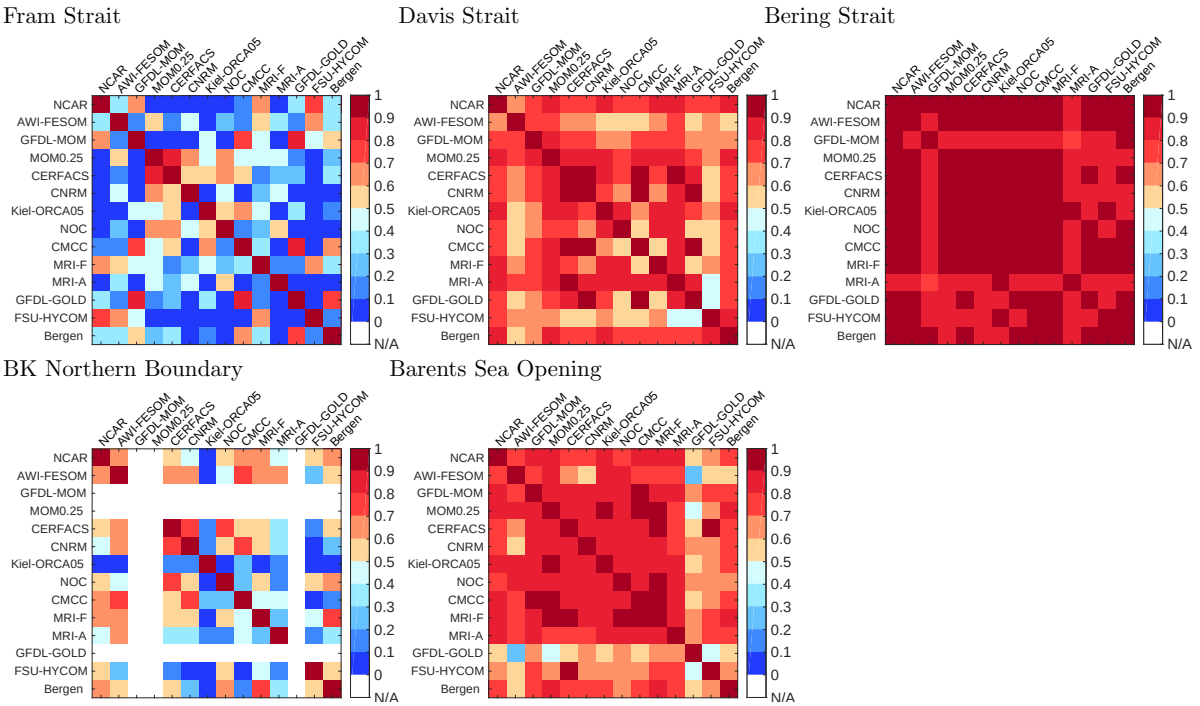

Figure 1: Correlation coefficients between models for freshwater transport at the Arctic gateways. The last 30 years (1978 - 2007) are used in the analysis. BKN data are not available in GFDL-MOM, MOM0.25 and GFDL-GOLD.

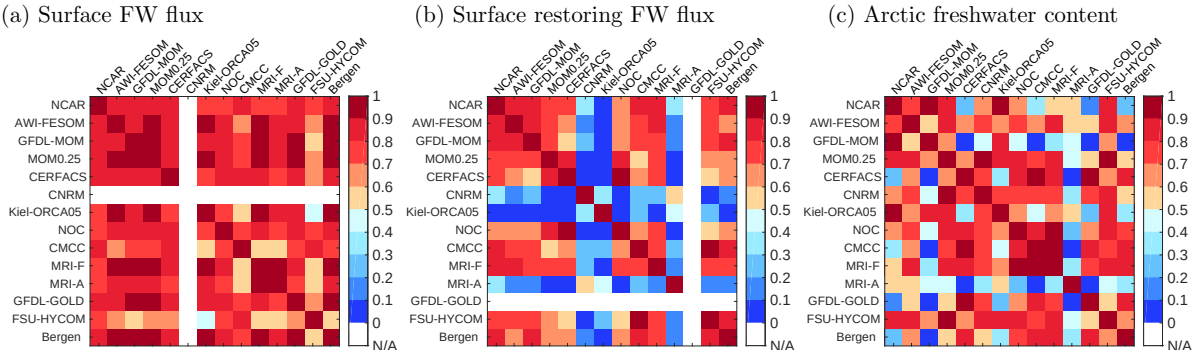

Figure 2: Correlation coefficients between models for Arctic (a) surface freshwater (FW) flux, (b) surface restoring FW flux and (c) freshwater content (FWC). The last 30 years (1978 - 2007) are used. The data for CNRM surface FW flux and GFDL-GOLD surface restoring FW flux are unavailable.

Herbaut, 2011; McGeehan and Maslowski, 2012; Wekerle et al., 2013; Stewart and Haine, 2013; Lu et al., 2014)). The robustness of conclusions derived from numerical models depends on the fidelity of model results. Here we analyze the ocean transport at Davis Strait to answer one particular question: Can we get a consistent conclusion on the driving mechanism for the Davis Strait FW export variability from the suite of models studied here? As the interannual variability of FW transport at Davis Strait is mainly determined by that of ocean volume transport, we will only discuss the ocean volume transport below. Note that the ocean volume transport is largely the same at Davis Strait and the CAA (small difference can be induced by surface water masses in Baffin Bay). When we discuss the FW budget of the Arctic Ocean, we have defined export transport to be negative. For the convenience of the following discussion, we define the southward volume transport at Davis Strait (export flux) to be positive.

As found in previous studies, the interannual variability of CAA ocean volume export is determined by sea surface height (SSH) gradients between the two ends of the CAA straits (Kliem and Greenberg, 2003; Jahn et al., 2010a,b; Houssais and Herbaut, 2011; Wekerle et al., 2013). On the Arctic Ocean side, the variation of large scale anticyclonic atmospheric circulation changes the storage of FW in the Beaufort Gyre (BG), leading to opposite changes of SSH in the BG and at the CAA coast (Proshutinsky et al., 2002). The SSH variation downstream of the CAA can be induced by changes of air-sea heat fluxes in the Labrador Sea (Houssais and Herbaut, 2011; Wekerle et al., 2013). Both the SSH variations upstream and downstream CAA can be partly explained by a common large scale atmospheric circulation characterized by the AO or NAO (Proshutinsky et al., 2002; Jahn et al., 2010a,b; Houssais and Herbaut, 2011; Wekerle et al., 2013). Here we will compare how the simulated ocean volume transport correlates with SSH and the AO index.

Model results

Wekerle et al. (2013) compared the two major CAA straits in their high resolution model simulations and found that the volume transport through Parry Channel (the west passage in the CAA) is strongly correlated with the SSH at both sides of the passage, but the transport through the Nares Strait (the east passage) is only determined by the SSH at the exit side. Because the SSH on both sides of CAA can be influenced by the same large scale atmospheric forcing, the volume transports through the two straits are well correlated with each other. Due to the variety in the number of straits and their detailed treatment in the models, we only focus on the total volume transport calculated at the Davis Strait. Figure 3 shows the correlation between the annual mean Davis Strait volume transport and the SSH for each model. The transport is positively correlated with the SSH along the coast of the Canadian Basin, and anti-correlated with the SSH in the Labrador Sea and the eastern Baffin Bay in all models, as suggested in the studies mentioned above. However, the strength of correlation varies in the models. High correlation is found north of Parry Channel in all the models, but the correlation is very different on the Lincoln Sea continental shelf.

Figures 4a,b,c show the correlation of annual mean volume transport with annual mean SSH on both sides of CAA and with the gradient (their difference). The SSH on the Arctic side is taken at the entrance of the Parry Channel, and on the downstream side we choose the location along the western Greenland coast in the Labrador Sea (see the caption in Figure 4). The models agree on strongest (anti-) correlation at zero time lag. The (anti-) correlation is significant for both upstream and downstream SSH, although the spread of correlation coefficients is larger for the upstream SSH. On average, the volume transport is more strongly correlated with the SSH difference between the two locations than with the SSH at either location. The mean correlation coefficient of volume transport with the SSH gradient is 0.93 among the models.

MOM0.25 has the lowest correlation coefficient between the volume transport and the SSH gradient (about 0.7). It is obviously different from other models in that its volume transport variability is more correlated with the downstream SSH rather than the SSH gradient. The SSH at the entrance of Nares Strait is anti-correlated with the Davis Strait volume transport in MOM0.25 (and a few other models, too). Therefore it is not appropriate to use the SSH gradient by taking the SSH north of Parry Channel on the Arctic side to explain the variation of volume transport component through the Nares Strait. In particular, MOM0.25 has a widened Nares Strait (the strait is 27.7 km wide in reality, but the model has 5 velocity grid cells at about 12 km resolution across the strait), so it might have too large contribution to the total volume export. This might explain why MOM0.25 has low correlation between the Davis Strait volume transport and the SSH gradient as we defined here. We leave this speculation to be verified in future work. Efforts are required to understand why the models have less agreement on the response

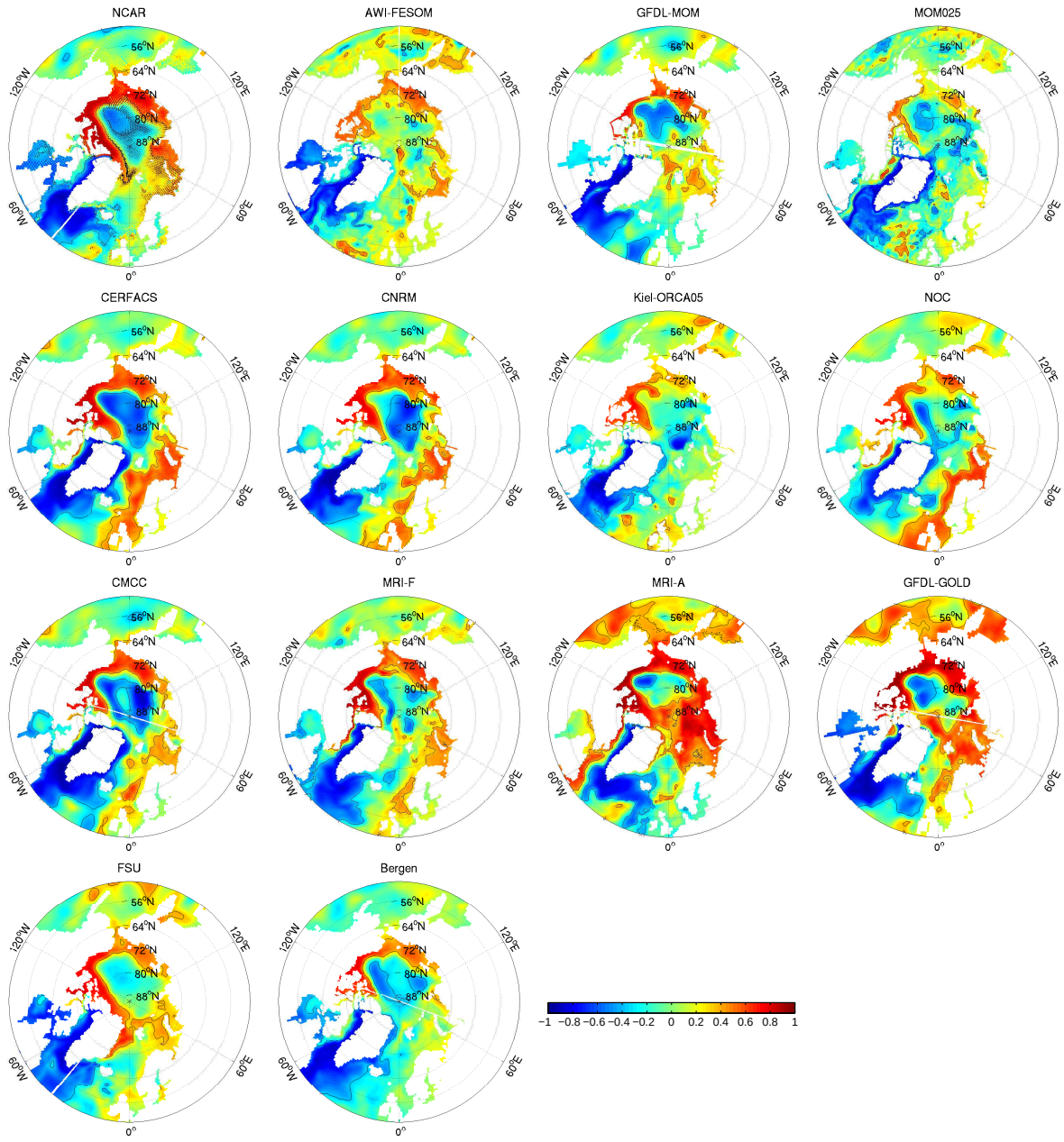

Figure 3: Correlation of annual mean Davis Strait volume transport with annual mean sea surface height (SSH) at zero time lag. Black contours indicate areas with the 95% confidence level. The last 30 years (1978 - 2007) are used in the calculation. Note that the southward volume transport (export) is defined to be positive.

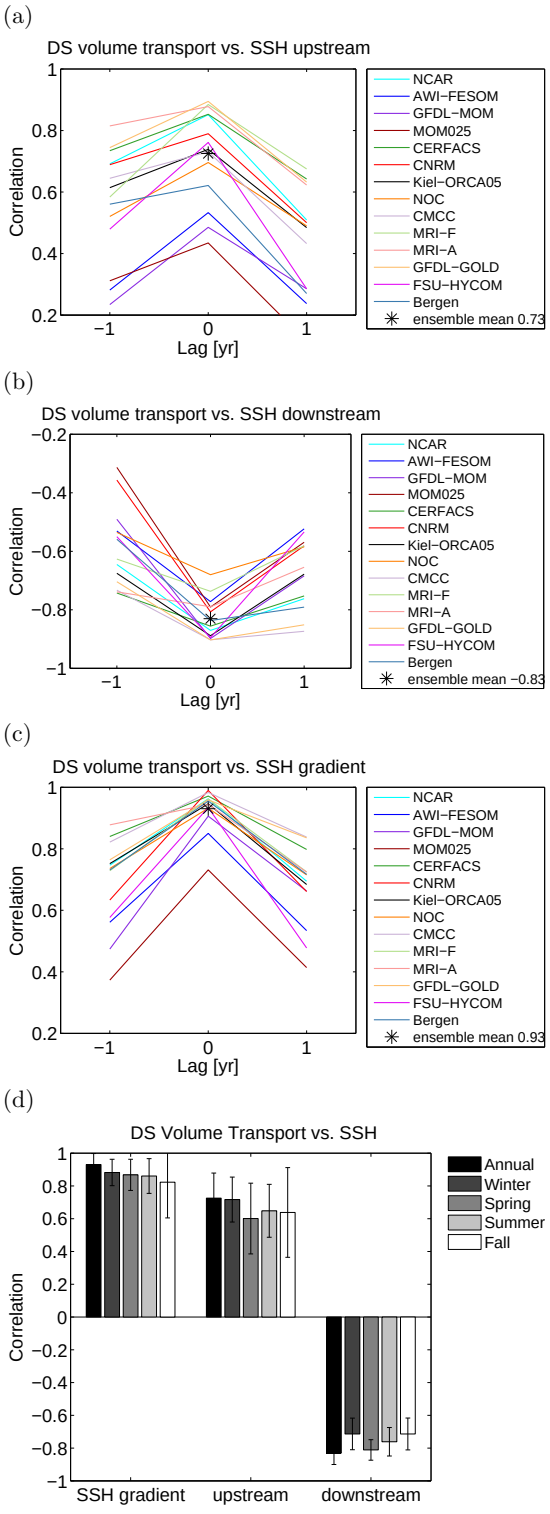

Figure 4: (a) Correlation of the Davis Strait volume transport with (a) upstream SSH on the Arctic side, (b) downstream SSH on the Labrador Sea side, and (c) the SSH difference. The means of correlation coefficients are shown with asterisk. (d) The mean correlation coefficients between the Davis Strait volume transport and the SSH at the zero lag for all models. In (d) the standard deviation of the model results are shown with error bars; the mean correlation coefficients are calculated for the annual mean and each season as well. All the correlations at the zero lag are significant at the 95% confidence level. The upstream SSH is taken in a 2° wide box at the entrance of Parry Channel; the downstream SSH is taken in a 2° wide box around (50°W, 61°N) at the western Greenland coast in the Labrador Sea. The last 30 years (1978 - 2007) are used in the calculation. Note that the southward volume transport (export) is defined to be positive.

(a) Correlation of DS transport with SLP (b) Correlation of DS transport with AO

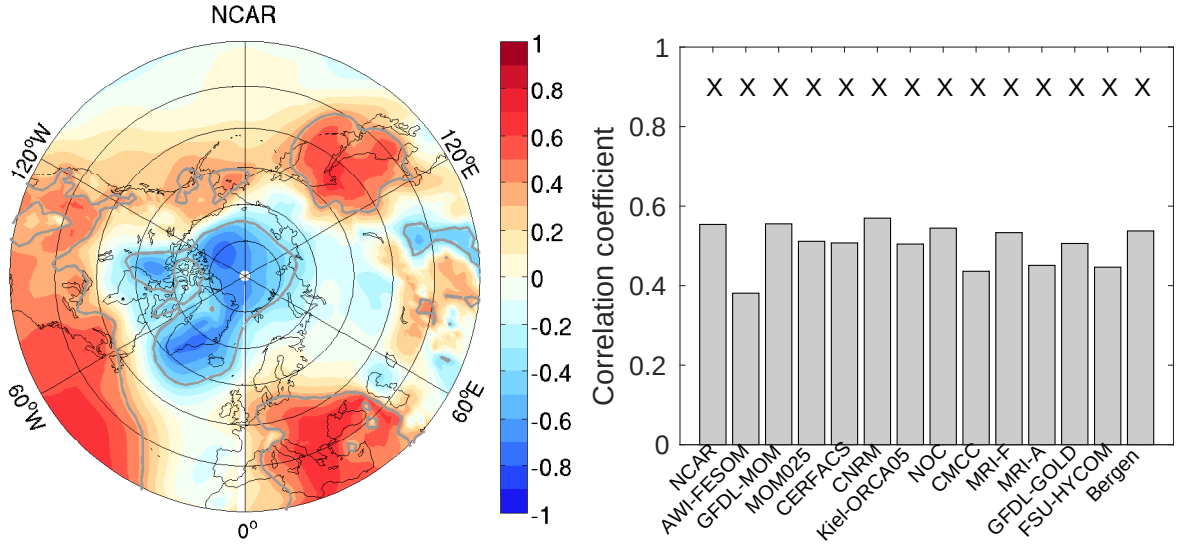

Figure 5: (a) Correlation between Davis Strait volume transport in NCAR and sea level pressure (SLP). Gray contours indicate areas of 95% significance. (b) Correlation coefficients between Davis Strait volume transport and Arctic Oscillation (AO) index. The cases at the 95% significance level are indicated with a cross 'X' on top of the bars. The last 30 years (1978 - 2007) are used in the calculation. The assimilation model MRI-A is not used in the calculation of the model ensemble mean. Note that the southward volume transport (export) is defined to be positive.

of volume transport to the SSH in the Lincoln Sea region, in order to reduce model spread and bias. For this purpose the CAA straits should be analyzed separately.

It is suggested in a model study that the control of SSH on the volume transport can vary with seasons (Lu et al., 2014). The correlation for each season is shown in Figure 4d. With the ensemble of models studied here, we find that the control of the SSH and SSH gradient on the ocean volume transport is not significantly different between seasons, because the difference of mean correlation coefficients between seasons is within the model spread.

The map of correlation coefficients between annual mean Davis Strait volume flux and sea level pressure (SLP) for one model (NCAR) is shown in Figure 5a. Because this map is very similar among the models, we only show one. Figure 5a is also very similar to the result based on a coupled climate model shown by Jahn et al. (2010b). The correlation pattern shows two characteristic features of the AO, with which the variability of the CAA outflow can be connected: the strong negative correlation over the western Arctic is associated with the variation of anticyclonic circulation in this region, and the gradient between the Greenland low and North Atlantic high is associated with the variation of westerly winds in the Labrador Sea region. When AO is in a positive phase, wind in the western Arctic is in a cyclonic regime, which reduces FWC and SSH in the BG and raises SSH along the American coast (Proshutinsky et al., 2002), thus increasing the export through CAA; at the same time, the westerly winds are intensified, leading to cooling in the Labrador Sea and SSH reduction (Lohmann et al., 2009), thus also increasing the export through the CAA (Houssais and Herbaut, 2011; Wekerle et al., 2013). When the AO is in a negative phase, the SSH anomalies on both sites will contribute to the reduction of the CAA export. The correlation between the Davis Strait ocean volume transport and the AO index is shown in Figure 5b. The correlation coefficients are significant in all models, but only with moderately high values (ranging from about 0.4 to 0.6). Therefore, other atmospheric and oceanic processes, on both sides of the CAA, also contribute to the variability of the export. In particular, the atmospheric circulation (cyclonic/anticyclonic) regimes characterized by the (negative/positive) anomaly of the Beaufort High sea-level pressure are linked not only to the AO, but also to other modes of atmospheric variability (Serreze and Barry, 2011).

On the seasonal time scale, the volume transport at the Davis Strait is also well correlated with the SSH gradient in most of the models, but not with the SSH on any side of the CAA (not shown). It implies that processes controlling the SSH seasonality upstream and downstream the CAA are different. Note that the seasonal variability of FW transport at Davis Strait is different from the CAA volume

transport due to the salt flux modification of the WGC (see discussions in Section 4).

To summarize: The models consistently support the findings of previous studies about the impact of large scale atmospheric circulation on the interannual variability of SSH and the Davis Strait export. Future research is required to understand, for example, how realistically the SSH variation in the Lincoln Sea region is simulated in the models, and whether its fidelity can impact on the simulated variability of ocean volume export through Nares Strait.

References

Condron, A., Winsor, P., Hill, C., Menemenlis, D., 2009. Simulated Response of the Arctic Freshwater Budget to Extreme NAO Wind Forcing. Journal of Climate 22, 2422–2437.

Houssais, M.N., Herbaut, C., 2011. Atmospheric forcing on the Canadian Arctic Archipelago freshwater outflow and implications for the Labrador Sea variability. Journal of Geophysical Research-oceans 116, C00D02.

Jahn, A., Tremblay, B., Mysak, L.A., Newton, R., 2010a. Effect of the large-scale atmospheric circulation on the variability of the Arctic Ocean freshwater export. Climate Dynamics 34, 201–222.

Jahn, A., Tremblay, L.B., Newton, R., Holland, M.M., Mysak, L.A., Dmitrenko, I.A., 2010b. A tracer study of the Arctic Ocean's liquid freshwater export variability. J. Geophys. Res. - Oceans 115, C07015.

Kliem, N., Greenberg, D.A., 2003. Diagnostic simulations of the summer circulation in the Canadian Arctic Archipelago. Atmosphere-ocean 41, 273–289.

Lohmann, K., Drange, H., Bentsen, M., 2009. Response of the North Atlantic subpolar gyre to persistent North Atlantic oscillation like forcing. Climate Dynamics 32, 273–285.

Lu, Y., Higginson, S., Nudds, S., Prinsenberg, S., Garric, G., 2014. Model simulated volume fluxes through the Canadian Arctic Archipelago and Davis Strait: Linking monthly variations to forcing in different seasons. Journal of Geophysical Research-oceans 119, 1927–1942.

McGeehan, T., Maslowski, W., 2012. Evaluation and control mechanisms of volume and freshwater export through the Canadian Arctic Archipelago in a high-resolution pan-Arctic ice-ocean model. J. Geophys. Res. 117, C00D14.

Peterson, I., Hamilton, J., Prinsenberg, S., Pettipas, R., 2012. Wind-forcing of volume transport through Lancaster Sound. Journal of Geophysical Research-oceans 117, C11018.

Prinsenberg, S., Hamilton, J., Peterson, I., Pettipas, R., 2009. Observing and interpreting the seasonal variability of the oceanographic fluxes passing through Lancaster Sound of the Canadian Arctic Archipelago, in: Nihoul, J. (Ed.), Influence of Climate Change on the Changing Arctic and Sub-Arctic Conditions, Springer. pp. 125–143.

Prinsenberg, S.J., Hamilton, J., 2005. Monitoring the volume, freshwater and heat fluxes passing through Lancaster Sound in the Canadian Arctic Archipelago. Atmosphere-ocean 43, 1–22.

Proshutinsky, A., Bourke, R.H., McLaughlin, F.A., 2002. The role of the Beaufort Gyre in Arctic climate variability: Seasonal to decadal climate scales. Geophysical Research Letters 29, 2100.

Serreze, M.C., Barry, R.G., 2011. Processes and impacts of Arctic amplification: A research synthesis. Global and Planetary Change 77, 85–96.

Stewart, K.D., Haine, T.W.N., 2013. Wind-driven Arctic freshwater anomalies. Geophys. Res. Lett. 40, 6196–6201.

Wekerle, C., Wang, Q., Danilov, S., Jung, T., Schröter, J., 2013. The canadian arctic archipelago throughflow in a multiresolution global model: Model assessment and the driving mechanism of interannual variability. J. Geophys. Res. - Oceans 118, 4525–4541.